Phase-transparency model of an eye optical system

V. V. Molebny[a], I. H. Chyzh[a], V. M. Sokurenko[a],
S. V. Molebny[a], I. G. Pallikaris[b], L. P. Naoumidis[b]

[a]Institute of Biomedical Engineering, 5 Dimitrov St., 252006 Kiev, Ukraine
[b]Eye Vardinoyannion Institute of Crete, University of Crete, 71110 Heraklion, Greece

ABSTRACT

Measurement of refraction distribution in the human eye opens new opportunities to make photorefractive surgery more accurate due to accounting imperfections not only of the cornea, but of the eye as an optical system. To calculate the to-be-ablated cornea layers, mathematical relations must be found between measured coordinates of retina ray tracings and transfer function of an eye. A new concept for modelling eye optical system is proposed using four phase transparencies, each of them exercising its own function: accommodation (equivalent to varifocal system), image focusing on the retina (optical system with constant optical power), regular aberrations (spherical and chromatic, astigmatism), and irregular phase distribution. It is shown, how the parameters, necessary for phase transparencies description, can be derived from direct and indirect measurements. Results of modelling experiment with simplified set of test points showed good sight correction. Investigated methodology proved to be fruitful even with limited number of test points and restricted length of polynomial approximation. In our refraction mapping system, transfer function reconstruction will use initial information from 65 points.

Keywords: eye model, phase transparency, retina ray tracing technique.

1. INTRODUCTION

Optical eye models have been evolved from simplest ones that predict the first-order properties of biologic eyes to higher-order models that include proper aberration content[1–13]. The simplest models represent a series of eye structure elements (cornea, lens and media), that describe paraxial ray traces. All surfaces are spherical, optical media are homogeneous, i. e., their refractive indices do not vary in space. Such models are only approximations, they do not reflect all eye peculiarities, even if the eye is emmetropic. Further model development was oriented on asphericization of cornea and lens surfaces and taking into account complex lens structure. Lotmar[4] modified Gullstrand's and Le Grand's eye models[1, 3] by introducing aspherics for description of the anterior surface of the cornea and posterior surface of the lens. The asphericity of the cornea was determined keratometrically, and the asphericity of the posterior lens surface was varied to match the measured spherical aberration.

El Hage and Berny proposed a similar model[5], except asphericity variance of both lens surfaces to match the measured spherical aberration. Corneal topography was determined experimentally by using photokeratoscope. After several attempts to approximate lens profile of the model, that could match spherical aberration of a real eye, hyperbola was taken as a meridian section of the anterior surface of the crystalline lens. An equation of the posterior surface was dependent on the accuracy of spherical aberration's approximation[5]. The Kooijman's eye model[6] also has all surfaces aspheric. Anterior and posterior cornea surfaces are ellipsoids, anterior lens surface is hyperboloid and posterior lens surface is paraboloid. Determination of asphericity coefficients is based on modelled matching and real retinal illumination distributions rather than on approximation to real aberrations. The corresponding model[7] accounts Stiles-Crawford effect (reduction in the perceived visual response by retina as a function of increasing angle of incidence of light).

For inclined wave fronts, these models do not work. Therefore, models were developed introducing the lens with refraction index varying in radial direction[8, 9]; or having multilayer composition[10–13]. Physiological aberrations have been measured by several authors independently[14, 15], and showed that:

Further information for correspondence –

V.V.M.: Email: molebny@quantum.kiev.ua
L.P.N.: Email: naoumidi@med.uch.gr

- physiological aberrations do not match with aberrations of ideally modelled optical system;
- transverse aberrations have significant differences even in the neighbouring zones at distances 1-2 mm;
- these differences of refraction are of the order of two diopters;
- aberrations' value and aberrations' distribution are not in accurate dependence with the degree of myopia or hyperopia;
- dispersion of refraction is inversely proportional to sight acuity.

Unfortunately, no one among the known models fits the case of non-homogeneous and irregular refraction distribution inside the eye. These models deal with centered surfaces, homogeneous media or regular spatial distribution of refraction index. First-order models fail to take into account eye aberrations. Higher-order models do it, but aberrations of the periphery ring zones of the pupil are difficult to be calculated. The more complicated model, the higher is the role of the parameters, measured directly on the live eye. In our approach, we tried to overcome the difficulties that arise in eye structure description. We propose phase-transparency model, that fits the needs of retina ray-tracing technique.

2. PHASE-TRANSPARENCY MODEL

It is well known that optical system of the eye implements the following functions: image forming on retina; accommodation, due to variations of optical power of eye's elements; and illuminance control, due to variations of iris diameter in the process of eye's accommodation to luminous field. These eye's functions could be executed by four thin plates - phase transparencies (fig. 1). The first and the second transparencies carry out the function of reshaping the wave front, i. e., phase distribution in the propagating electromagnetic wave, in such a way as to transform its shape from a convex or plane type to a concave type. In this case, front's normals (rays) intersect the retina in a single point. The first phase transparency is equivalent to varifocal system (for accommodation), and the second - to optical system with constant optical power (for image focusing on the retina).

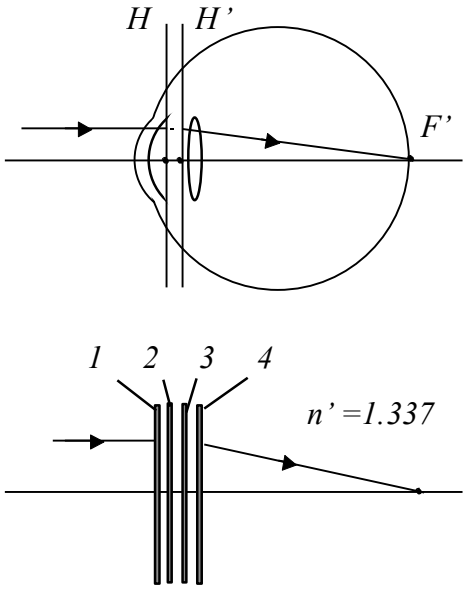

Fig. 1. Modelling an optical system of an eye with phase transparencies

The third and fourth transparencies model a kind of counteraction to the first two transparencies in carrying out their actions. The third phase transparency represents regular spherical aberrations, regular astigmatism, and chromatic aberrations. The fourth phase transparency models irregular influence on the phase of a wave, propagating through the eye. It describes irregular aberrations, resulting from natural imperfections of a real eye.

Accommodation transparency - phase transparency #1. The first phase transparency models varifocal optical component (i. e., optical component with variable focal length) without aberrations. Its task is to transform a convex wave front into the plane front, which then enters the second transparency. Radius of a convex spherical wave is restricted by distances of far and near points of clear sight. For normal eye, it is an interval from -∞ to -90 mm. During the human life, the depth of accommodation is being reduced. Distance a_n in fig. 2 indicates the distance from an eye to the near point of clear sight, and distance a_f - to the far point.

As it can be seen from fig. 2, the accommodation phase transparency introduces a zero phase shift for axial ray, and some positive shift at the periphery:

$$\Delta\Phi_1(h) = -k \cdot n'a \cdot \left(\sqrt{1 + \frac{h^2}{a^2}} - 1 \right), \tag{1}$$

where $\Delta\Phi_1(h)$ is a phase shift, h is a distance from axis to a ray, $k = 2\pi/\lambda$ is a wave number, a is a radius of a convex spherical wave, i. e., the distance from eye to object of sight fixation. According to the rule of sign, distance a in the expression (1) has the sign "–". Distance a varies from -∞ to -90 mm in normal eye, and from a_n to a_f in the eye with reduced depth of accommodation.

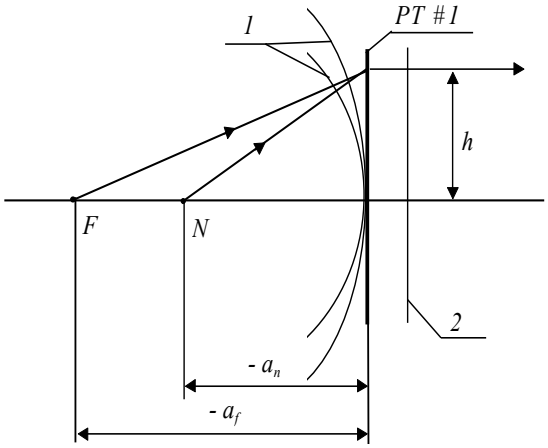

Fig. 2. Phase transparency # 1: *1* - wave front before the transparency,
2 - wave front after having passed the transparency

Refraction transparency - phase transparency #2. The second transparency models the refraction of an eye without aberrations, when a plane wave enters an eye, i. e., it is accommodated for infinity. In this case, the transparency transforms the plane front into a concave spherical front (fig. 3) with zero phase shift on the axis and positive phase shift at the periphery:

$$\Delta\Phi_2(h) = k \cdot n'a' \cdot \left(\sqrt{1 + \frac{h^2}{a'^2}} - 1 \right), \tag{2}$$

where n'=1.337 is the refractive index of vitreous.

If an eye is emmetropic, then point *F'* coincides with the retinal surface. If ametropic, then this point will be in front of the retina (in the case of myopia) and behind the retina (in the case of hyperopia). The above expression can be rewritten as follows:

$$\Delta\Phi_2(h) = k \cdot n' a'_0 \cdot q \cdot \left(\sqrt{1 + \frac{h^2}{a'^2_0 \cdot q^2}} - 1 \right), \tag{3}$$

where $q = 1 + \frac{\Delta a'}{a'_0}$ is a parameter of ametropic eye.

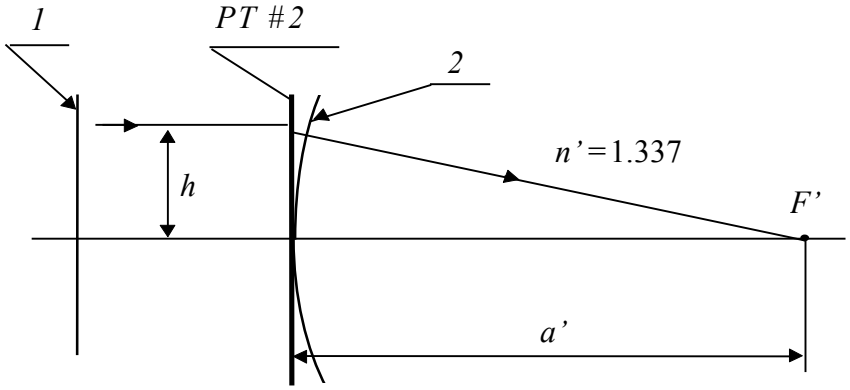

Fig. 3. Phase transparency # 2: *1* - wave front before the transparency,
2 - wave front after having passed the transparency

Aberration transparency - phase transparency #3. Unlike previous transparencies, phase transparency #3 describes the deviation of wave front from regular spherical form. Aberrations are supposed to be regular, i. e. they can be expanded into power series relatively to ray coordinates. Phase shift, caused by the transparency #3, may be computed using the function of wave aberration. In fig. 4*a*, wave aberration $W_{nm}(\rho, \varphi)$ is shown as a distance between wave front W_3 of the third phase transparency and spherical wave front W_{1+2}, formed by transparencies #1 and #2. Phase shift $\Delta\Phi_3(\rho, \varphi)$, caused by the third transparency, is defined as follows:

$$\Delta\Phi_3(\rho, \varphi) = k \cdot n' \cdot W_{nm}(\rho, \varphi), \tag{4}$$

where ρ and φ are polar coordinates in the plane of transparency #3, $W_{nm}(\rho, \varphi)$ is wave front function that may have no central or axial symmetry.

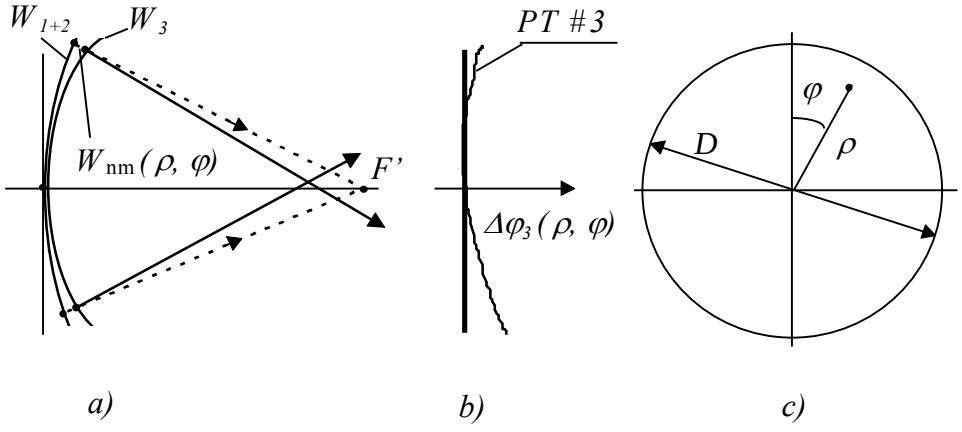

Fig. 4. Phase transparency # 3: W_{1+2} is a spherical front, having its center in point *F'*,
W_3 is a wave front, deformed by aberrations, *W* is wave aberration, *D* is the diameter of the pupil

Transparency of irregular aberrations - phase transparency #4. Irregular aberrations (fig. 5) are the result of optical non-homogeneity of eye media and local deformations of eye's optical surfaces. These aberrations are specific for each individual and can be different for left and right eyes. Irregular aberrations are difficult to be expanded into power series. Function of phase shift $\Delta\Phi_4(y, x)$ is defined by difference between actual wave aberration $W(\rho, \varphi)$ of the real eye and function of regular wave aberration $W_{nm}(\rho, \varphi)$, being modelled by the third phase transparency:

$$\Delta\Phi_4(y, x) = k \cdot n' \cdot \left[W(\rho, \varphi) - W_{n\,m}(\rho, \varphi)\right], \tag{5}$$

where $y = \rho \cdot \cos\varphi, \quad x = \rho \cdot \sin\varphi$.

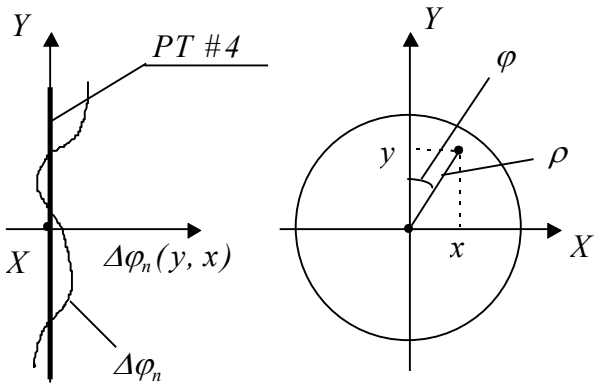

Fig. 5. Phase transparency # 4

Function $W(\rho, \varphi)$ can be got only experimentally by measuring local eye refraction or distribution of transversal aberrations. Orthogonal coordinates *y, x* are preferable for presentation of function $\Delta\Phi_4$, because its 3D graph has local maxima and minima ("hills" and "valleys") without any symmetry, and therefore, it is more convenient for interpolation in orthogonal system of coordinates.

3. EVALUATION OF MODEL PARAMETERS

To evaluate transfer function of an eye, all components must be summed up:

$$\Delta\Phi(y, x) = \Delta\Phi_1 + \Delta\Phi_2 + \Delta\Phi_3 + \Delta\Phi_4 . \tag{6}$$

From $\Delta\Phi(y, x)$, pupil function is determined, as well as the topography of the to-be-ablated cornea layers. Optical system of an eye is shown in fig. 6 as a set of phase transparencies. Two rays pass through it. One of them is an axial ray, another ray is an arbitrary-inclined ray with coordinates ρ, φ or *y, x* at the plane of transparencies.

It is well known that image *A'* will not be distorted by aberrations, if the first and second rays reach the point *A'* with the same eikonal value. The phase increment is equal to $2\pi(n'a' - a) / \lambda$ for axial ray and $2\pi\left[-a - \Delta + (\Delta' + a') \cdot n' + \Delta\Phi(y, x)\right]$ for inclined ray. Both increments are equal to each other, if $-\Delta + n' \cdot \Delta' = \Delta\Phi(y, x)$, or

$$W_z(y, x) = \Delta\Phi(y, x) - (n'\Delta' - \Delta) = 0 , \tag{7}$$

where $W_z(y, x)$ is the phase component of pupil function[16].

Substituting expression (6) into (7), one can get

$$W_z(y,x) = (\Delta\Phi_1 + \Delta) + (\Delta\Phi_2 - n' \cdot \Delta') + \Delta\Phi_3 + \Delta\Phi_4 . \tag{8}$$

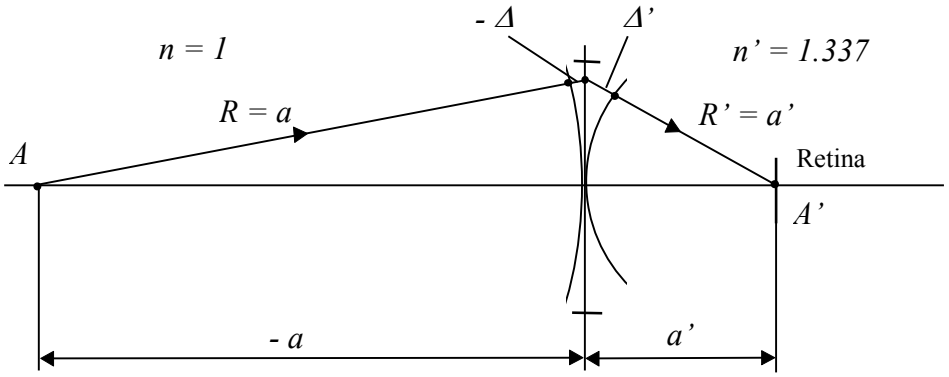

Fig. 6. Evaluation of transfer function

If $\Delta\Phi_1 + \Delta \neq 0$, it means that point A is located outside the accommodation limits of an eye. If $\Delta\Phi_2 - n' \cdot \Delta' \neq 0$, it indicates that the eye is ametropic. The sum of both brackets of (8) equals zero, when ametropia is compensated by additional accommodation effort. If the sum of these brackets in real eye does not equal zero, additional phase transparency must be inserted, i. e., lens (glasses or contact lens), or the cornea surface must be ablated to obtain sharp image of the point A.
A similar procedure of compensation must be done as well, when $\Delta\Phi_3 \neq 0$ and $\Delta\Phi_4 \neq 0$. Thus, when condition (7) is not implemented, it is necessary to add some term $\Delta\Phi_r(y, x)$ into (7):

$$\Delta\Phi_r(y, x) = -W_z(y, x) , \tag{9}$$

i. e., additional phase transparency should be inserted, whose phase component is identical to that of the pupil function, but having the opposite sign.

Function $\Delta\Phi_r(y, x)$ simplifies computations of the topography of the to-be-ablated layers of the cornea, because their thickness is proportional to $\Delta\Phi_r(y, x)$. In this way, aberrations, as well as ametropia, may be corrected.

Pupil function $f(y, x)$, used for computations of the most important characteristics of sight, is defined as follows[16]:

$$f(y,x) = \tau^{1/2}(y, x) \cdot exp\left[-i \cdot W_z(y, x)\right], \qquad y, x \in \Omega \tag{10}$$

and

$$f(y, x) = 0, \qquad y, x \notin \Omega$$

where Ω is a hole zone of the exit pupil, $\tau(y, x)$ is a function of transmittance of an optical system in pupil coordinates, accounting Stiles-Grawford effect (if necessary).

Point spread function (PSF) $e(y', x')$ is calculated as[16]:

$$e(y', x') = \left| F^{-1}\left[f(y, x) \right] \right|^2, \tag{11}$$

where y', x' are coordinates in the plane of retina.

Optical transfer function (OTF) is defined as Fourier transform of PSF or as autocorrelation of pupil function:

$$\begin{aligned} D(\nu_y, \nu_x) &= \frac{1}{B} \iint\limits_{S(y_0, x_0)} f(y, x) \cdot f(y - y_0, x - x_0)\, dy\, dx = \\ &= \frac{1}{B} \iint\limits_{S(y_0, x_0)} \tau^{1/2}(y, x) \cdot \tau^{1/2}(y - \nu_y \lambda, x - \nu_x \lambda) \cdot exp\left[i \cdot (W_z(y, x) - W_z(y - \nu_y \lambda, x - \nu_x \lambda)) \right] dy\, dx \end{aligned} \tag{12}$$

where $B = \iint\limits_{\Omega} \tau(x, y)\, dy dx$, $y_0 = \nu_y \lambda$, $x_0 = \nu_x \lambda$; $S(y_0, x_0)$ - see fig. 7; ν_y, ν_x are spatial frequencies on axis *oy* and *ox*, λ is a wavelength.

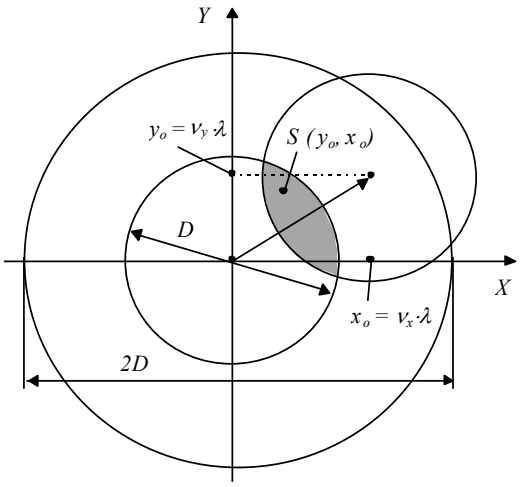

Fig. 7. Evaluation of the OTF using auto-correlation of pupil function

Note, that y_0 and x_0 (fig. 7), i. e., coordinates of the center of shifted pupil contour, are limited by the value of 2*D*, where *D* is a diameter of exit pupil. Then, the maximum values of y_0 and x_0 are equal to *D*. Therefore, the highest value of angular spatial frequency is

$$\nu_{yl} = \nu_{xl} = D/\lambda$$

or, in image space (inside the eye):

$$\nu_{yl}' = \nu_{xl}' = D/n'\lambda = D/1.337 \cdot \lambda \,. \tag{13}$$

Hence, the highest linear spatial frequency in the retina plane equals to

$$N_{yl} = N_{xl} = \nu'_{yl}/a'_0 = \nu'_{xl}/a'_0 = \frac{D}{1.337 \cdot \lambda \cdot a'_0} \,. \tag{14}$$

Sight acuity is defined as value, inverse to ν_{yl} or ν_{xl}.

Equations (10), (11), and (8) are used to find the PSF defining the region of values of y', x', where relative level of irradiance is greater than a given value. These values restrict the space of focal region determining sight acuity and depth of sharp vision.

To determine transfer functions of phase transparencies, several parameters and functions are to be found, among them distances a_n and a_f, pupil average value of myopia or hyperopia, functions $W_{nm}(\rho, \varphi)$ and $W(\rho, \varphi)$. All of them can be obtained by direct or indirect measurements with investigated eye. Experimental setup for these measurements, its functional structure and principal concepts are described in our previous works[17, 18]. The essence of the method consists in determining wave functions from a set of data of measured declinations (in the plane of retina) of thin rays entering the eye in the points with known coordinates. Zernike polynomials are used for analytical expressions, describing wave functions.

4. EXPERIMENTAL RESULTS AND MODELLING

For our first experiments, we have chosen a limited number of test points in the polar system of coordinates. Totally, 16 points were tested, placed on two circles with diameters 3 mm and 5 mm (8 per circle). We measured the coordinates of crossings of the retina by thin laser rays entering the eye in predetermined 16 points. These data were used for wave and transfer functions evaluation. Refraction map of the eye in terms of focal power can be also reconstructed. We demonstrated this procedure for four typical cases of refraction non-homogeneity[17].

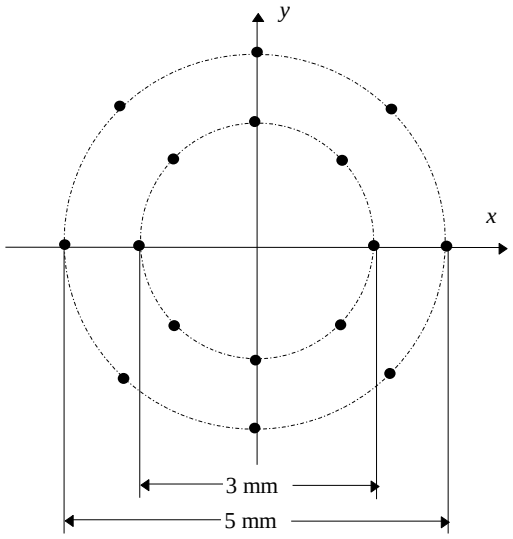

Fig. 8. Placement of test points in pupil coordinates

Transfer function, interpolated using Zernike polynomials, gave start for modelling ablation procedure with flying spot technology. The results of ablation modelling were then recomputed into retina ray crossing points for comparison with initial objective measurements. As an illustration, measurements and modelling on myopic eye are demonstrated by figures 8-12. Fig. 8 represents the placement of test points, where thin laser beams enter the eye (in parallel to sight axis). Fig. 9 shows positions of these beams' centroids on retina. Reconstructed refraction map in terms of focal power is shown in fig. 10. After interpolation, restricted by four-term polynomials, transfer function is got (fig. 11). Results of ablation modelling (in the form of retina crossing points) are demonstrated in fig. 12 (note, that coordinate scaling in figures 9 and 12 differ by an order).

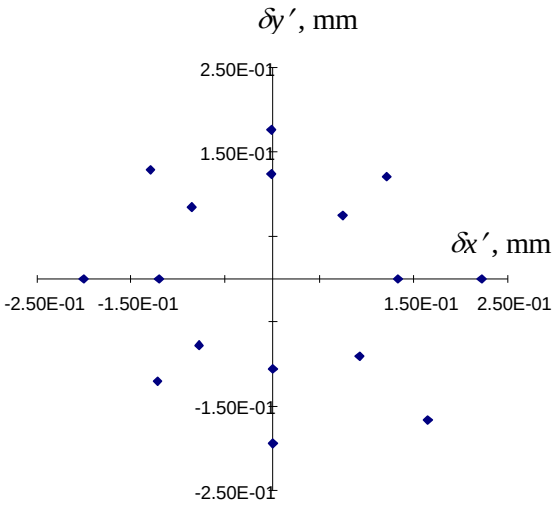

Fig. 9. Positions of beam centroids on retina

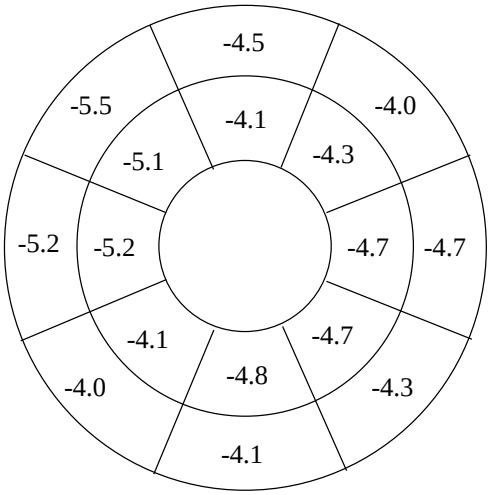

Fig. 10. Reconstructed refraction map (in diopters)

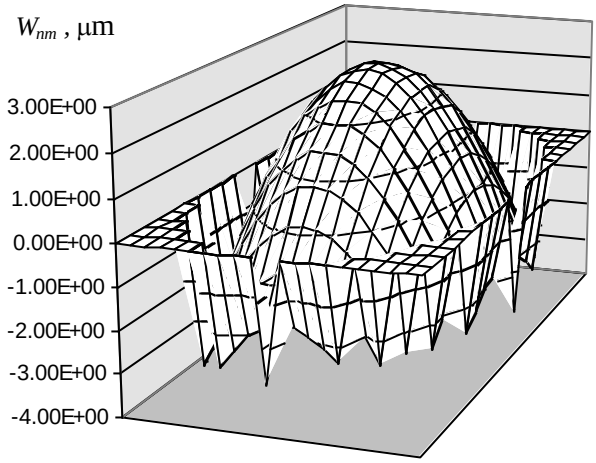

Fig. 11. Reconstructed transfer function

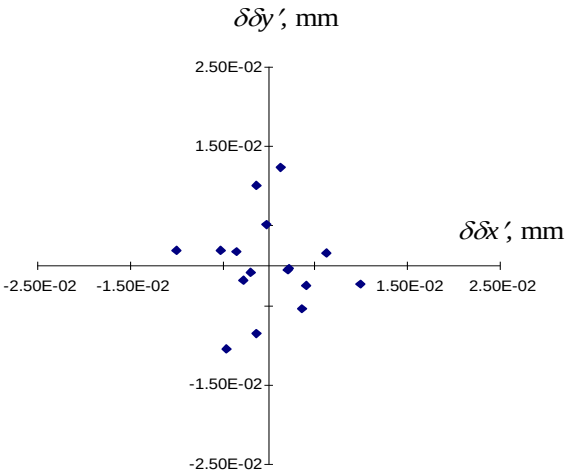

Fig. 12. Modelling of retina ray tracings after sight correction

5. DISCUSSION AND CONCLUSION

Measurement of refraction distribution in the human eye opens new opportunities to make photorefractive surgery more accurate due to accounting imperfections not only of the cornea, but of the eye as an optical system. Described here methodology of using phase-transparency model proved to be fruitful even with limited number of test points and restricted length of polynomial approximation. Our recent studies showed that the six-term Zernike approximation will be optimal issuing from the criterion “accuracy-computing resources”. In our refraction mapping setup, 65-point sensing will be used (one point is central plus 64 points placed on four circles).

ACKNOWLEDGEMENTS

This work was carried out with financial support of the STCU - Science and Technology Center in Ukraine (project No. 418) being funded by the governments of the United States, Canada, and Sweden. Initially, ideas of retina ray tracing methodology were discussed by Prof. V. V. Molebny with Prof. I. G. Pallikaris and Prof. L. P. Naoumidis in November 1994.

REFERENCES

1. A. Gullstrand, "Appendicle to part 1", in: H. von Helmholtz, *Physiological optics*, 3rd Edition, Vol. 1, Voss, Hamburg, pp. 350-358, 1909.
2. H. von Helmholtz, *Physiological optics*, 3rd Edition, Vol. 1, Voss, Hamburg, pp. 91-121, 1909.
3. Y. le Grand, S. G. el Hage, *Physiological optics*, Springer Verlag, Berlin, pp. 57-69, 1980.
4. W. Lotmar, "Theoretical eye model with aspherics", *J. Opt. Soc. Am.* **61**, pp. 1522-1569, 1971.
5. S. G. el Hage, F. Berny, "Contribution of the crystalline lens to the spherical aberration of the eye", *J. Opt. Soc. Am.* **63**, pp. 205-211, 1973.
6. A. C. Kooijman, "Light distribution on the retina of a wide-angle theoretical eye", *J. Opt. Soc. Am.* **73**, pp. 1544-1550, 1983.
7. R. Navarro, J. Santamaria, J. Bescos, "Accommodation dependent model of the human eye with aspherics", *J. Opt. Soc. Am.* **A2**, pp. 1273-1281, 1985.
8. J. W. Blaker, "Toward an adaptive model of the human eye", *J. Opt. Soc. Am.* **70**, pp. 220-223, 1980.
9. W. M. Rosenblum, J. W. Blaker, M. G. Block, "Matrix method for the evaluation of lens systems with radial gradient-index elements", *Am. J. Optometry: Physiol. Opt.* **65**, pp. 661-665, 1988.
10. O. Pomerantzeff, H. Fish, J. Govignon, C. Schepens, "Wide-angle optical model of the eye", *Opt. Acta* **19**, pp. 387-388, 1972.
11. O. Pomerantzeff, M. Pankratov, G. Wang, P. Dutault, "Wide-angle optical model of the eye", *Am. J. Optometry: Physiol. Opt*. **61**, pp. 166-176, 1984.
12. O. Pomerantzeff, M. Pankratov, G. Wang, "Calculation of an JOL from the wide angle optical model of the eye", *Am. Inter-Ocular Implant. Soc. J.* **11**, pp. 37-43, 1985.
13. I. H. Al-Ahdali, M. A. El-Messiery, "Examination of the effect of the fibrous structure of a lens on the optical characteristics of the human eye: a computer-simulated model", *Appl. Opt.* **34**, pp. 5738-5745, 1995.
14. M. S. Smirnov, "Measurement of the wave aberration of the eye", *Biophysics* (Moscow) **6**, pp. 776-794, 1961.
15. N. M. Sergienko, *Ophthalmological Optics* (in Russian), Meditsina Publ., Moscow, 142 pp., 1991.
16. S. A. Rodionov, *Automation of Optical Systems Design* (in Russian), Mashinostroenie, Leningrad, 269 pp., 1982.
17. V. V. Molebny, I. G. Pallikaris, L. P. Naoumidis, I. H. Chyzh, S. V. Molebny, V. M. Sokurenko, "Retina ray-tracing technique for eye-refraction mapping", *Proc. SPIE* **2971**, pp. 175-183, 1997.
18. *Electro-Optic Interferometric System for Ophthalmologic Investigations - EYEMAP*, Project # 418, First Annual Technical Report, Project Leader - V. V. Molebny, STCU - IBME, Kyiv, 57 pp., June 1997.